IOP PUBLISHING
IOP FTC
JOURNAL OF PHYSICS D: APPLIED PHYSICS
J. Phys. D: Appl. Phys. **46** (2013) 482001 (5pp)
doi:10.1088/0022-3727/46/48/482001

FAST TRACK COMMUNICATION

Coupling effects of driving frequencies on the electron heating in electronegative capacitive dual-frequency plasmas

A Derzsi[1], Z Donkó[1] and J Schulze[2,3]

[1] Institute for Solid State Physics and Optics, Wigner Research Centre for Physics, Hungarian Academy of Sciences, 1121 Budapest, Konkoly-Thege Miklós str. 29-33, Hungary
[2] Institute for Plasma and Atomic Physics, Ruhr University Bochum, 44780 Bochum, Germany
[3] Department of Physics, West Virginia University, Morgantown, WV 26506, USA

E-mail: derzsi.aranka@wigner.mta.hu

Received 20 August 2013, in final form 23 October 2013
Published 12 November 2013
Online at stacks.iop.org/JPhysD/46/482001

Abstract
The coupling effects of low-frequency (LF) and high-frequency (HF) driving sources on plasma parameters and electron heating dynamics are investigated in low-pressure electronegative capacitive discharges. Kinetic particle simulations reveal frequency coupling mechanisms different from those characteristic of electropositive discharges operated in α- and/or γ-mode due to the presence of the drift-ambipolar electron heating mode in electronegative plasmas. Here, the LF component affects the electron heating at the collapsing sheath and inside the plasma bulk, having consequences on the separate control of ion properties and the electronegativity of the plasma.

(Some figures may appear in colour only in the online journal)

Capacitively coupled radio frequency (CCRF) discharges have become widely used efficient tools for a variety of applications, ranging from plasma based etching and deposition procedures in the semiconductor industry to plasma assisted surface treatment of medical interest [1–3]. Extensive study of CCRF discharges has been, and still is, strongly motivated by the practical goal of clarifying the effect of external control parameters on process relevant plasma characteristics. Especially, the feasibility of the separate control of the ion flux and energy distribution at the substrate, which is crucial for applications, has been attracting particular attention. The realization of such control necessitates a detailed understanding of the complex physics of CCRF plasmas underlying the electron heating and ionization dynamics.

Electronegative plasmas are characterized by the presence of negative ions and, consequently, by the electronegativity $\zeta = \bar{n}_-/\bar{n}_e$, where $\bar{n}_-$ is the negative ion and $\bar{n}_e$ is the electron density averaged over the electrode gap. In the case of strongly electronegative plasmas ($\zeta \gg 1$), properties (e.g. discharge structure, particle densities, electron power balance) different from those of electropositive or weakly electronegative discharges have been reported [4, 5]. The different behaviour is attributed to the peculiarities of electronegative plasmas, such as the development of a high electric field in the bulk region [6] or the formation of double layers [7–10]. The strong bulk electric field was also found to affect the electron bounce resonance heating in electronegative plasmas [11, 12].

The heating of electrons and the corresponding ionization define the operation mode of the discharge. Electropositive CCRF discharges can operate in α-mode (at low pressures and driving voltages) [13], where the ionization is dominated by electrons accelerated by the oscillating sheaths. In γ-mode (at high pressures and/or voltages) [13], the ionization is dominated by secondary electron avalanches. At high pressures, e.g. in atmospheric pressure microplasmas, the ionization may be dominated by ohmic heating in the bulk (Ω-mode) [14]. In single-frequency (SF) discharges with high

electronegativity, the drift-ambipolar (DA) operation mode has recently been identified and its physical origin has been clarified [15]. In DA-mode, the ionization is dominated by electrons accelerated (i) by a strong drift field in the plasma bulk due to the low dc conductivity resulting from the depleted electron density and (ii) by an ambipolar field at the sheath edges caused by local maxima of the electron density in the electropositive edge region of the discharge. Depending on the choice of global control parameters such as the processing gas mixture, pressure, and voltage, CCRF plasmas can be operated in a hybrid combination of several modes.

A 'classical' method for achieving independent control of the ion properties at the electrodes is the simultaneous excitation of the discharge by two substantially different frequencies [16, 17]. In such dual-frequency (DF) discharges, the ion flux is expected to be tunable by the high-frequency (HF) voltage (due to the enhanced electron heating at high frequencies), while the ion energy is adjusted by the low-frequency (LF) voltage (by varying the mean sheath voltage). The efficiency of this method turned out to be reduced by the coupling of the driving frequencies in electropositive discharges [18–21]: the LF component, expected to control only the mean ion energy at the substrate, was found to affect both the flux and the mean energy of ions reaching the electrodes. The origin of this effect is the modification of the electron heating and ionization dynamics in the HF periods due to the modulation of the sheath width by the LF component.

In this paper we address the question: How do the different driving frequencies interact in electronegative discharges? Answering this question is important, since understanding the frequency coupling is essential to realize the optimum control of process relevant plasma parameters in electronegative gases such as CF_4, SF_6, SiH_4, BCl_3, F_2, Cl_2, O_2, which are frequently used for applications, e.g. plasma enhanced chemical vapour deposition and plasma etching [1–3]. The present investigations are based on the recent clarification of the electron heating and ionization dynamics in SF capacitive electronegative discharges operated in the DA-mode [15]. Our kinetic simulations of low-pressure DF CF_4 plasmas reveal two novel frequency coupling mechanisms, specific to electronegative discharges operated in the DA-mode or in a hybrid α-DA mode. Their physical origin and consequences on the separate control of the ion flux and mean energy at the electrodes as well as their influence on the electronegativity of the discharge are clarified.

The simulations are based on a one-dimensional in space, three-dimensional in velocity (1D3V) bounded electrostatic particle-in-cell (PIC) code complemented with Monte Carlo treatment of collision processes. The simulations are performed for an electrode gap of $d = 1.5$ cm. One of the electrodes is grounded, while a voltage waveform of $V(t) = V_{HF}\cos(2\pi f_{HF}t) + V_{LF}\cos(2\pi f_{LF}t)$ is applied to the other one. The frequencies are $f_{HF} = 27.12$ MHz and $f_{LF} = 1.937$ MHz, the voltage amplitudes, V_{HF} and V_{LF}, are varied at different pressures. The plasma species considered in the model are electrons, CF_3^+, CF_3^- and F^- ions. The gas temperature is fixed to 350 K. The cross sections and rate coefficients are taken from [22–24], the ion-induced secondary electron emission coefficient, γ, is set to 0.1, the probability of electron reflection from the electrodes is 0.2, the ion-ion ($CF_3^+ + CF_3^-$, $CF_3^+ + F^-$) recombination rate is 5.5×10^{-13} m^3 s^{-1} [25]. Details of the PIC simulation code for CF_4 can be found in [26, 27].

Figure 1 shows the frequency coupling in case of weakly electronegative plasmas at 10 Pa. In the first column, discharge characteristics corresponding to SF ($f_{HF} = 27.12$ MHz, $V_{HF} = 300$ V) excitation are presented, while in the second column results for DF ($f_{HF} = 27.12$ MHz, $f_{LF} = 1.937$ MHz, $V_{HF} = 300$ V, $V_{LF} = 100$ V) excitation are shown. In each column, spatiotemporal plots of the electron heating rate, ionization rate, electric field, electron density, and electron conduction current density are presented. The plots cover 516.26 ns corresponding to one LF period (14 HF periods). Under such conditions, both the SF and DF plasmas are characterized by a low electronegativity, 0.22 and 0.41, respectively. The discharge characteristics observed here are typical of SF and DF excited low-pressure electropositive plasmas operated in α-mode. Comparison of the results of the SF and the DF excitation reveals the 'classical' frequency coupling [18–21]: the HF sheath is pushed away from the electrode at times of large LF sheath; the HF sheath oscillates with a smaller velocity (due to increasing ion density towards the bulk); this results in less effective acceleration of electrons by the expanding sheath and, therefore, reduced ionization.

In figure 2, we show results obtained for the case of strongly electronegative plasmas at a higher pressure of 80 Pa. Again, simulation results are presented both for SF ($f_{HF} = 27.12$ MHz, $V_{HF} = 100$ V) excitation (first column) and DF ($f_{HF} = 27.12$ MHz, $f_{LF} = 1.937$ MHz, $V_{HF} = 100$ V, $V_{LF} = 200$ V) excitation (second column). Under these conditions, the electronegativity of the SF and DF discharges are 32.5 and 27.8, respectively. The high electronegativity is caused by enhanced electron attachment at higher pressures. In the first column, the discharge characteristics correspond to the DA operation mode of an electronegative discharge excited by a single HF source [15]: strong electron heating and ionization in the bulk plasma region and at the collapsing sheath edges are found to be dominant compared to the ionization by electrons accelerated by the expanding boundary sheaths; the electric field is high in the bulk (where the density of electrons is depleted), and at the collapsing sheath edges (where the gradient of the electron density is maximum); the electron conduction current density is maximum in the bulk. In this case, the spatiotemporal plots exhibit completely symmetric patterns within the two halves of any HF period. This behaviour is substantially altered when an LF source is applied simultaneously, as can be seen in the plots of the second column. For an explanation of these results, knowledge on the electron heating dynamics in the DA-mode operation is recalled.

In [15], an analytical model clarified that the electron heating in the DA mode is caused (a) by a drift field in the bulk region, $E_D = j/\sigma_{dc}$, where j is the electron current density and $\sigma_{dc} = (n_e e^2)/(m_e \nu_c)$ is the dc conductivity, and (b) by an ambipolar field at the sheath edges, $E_A = -kT_e/(en_e)(\partial n_e/\partial x)$, where n_e is the electron number density, e is the elementary charge, m_e is the electron mass, ν_c is

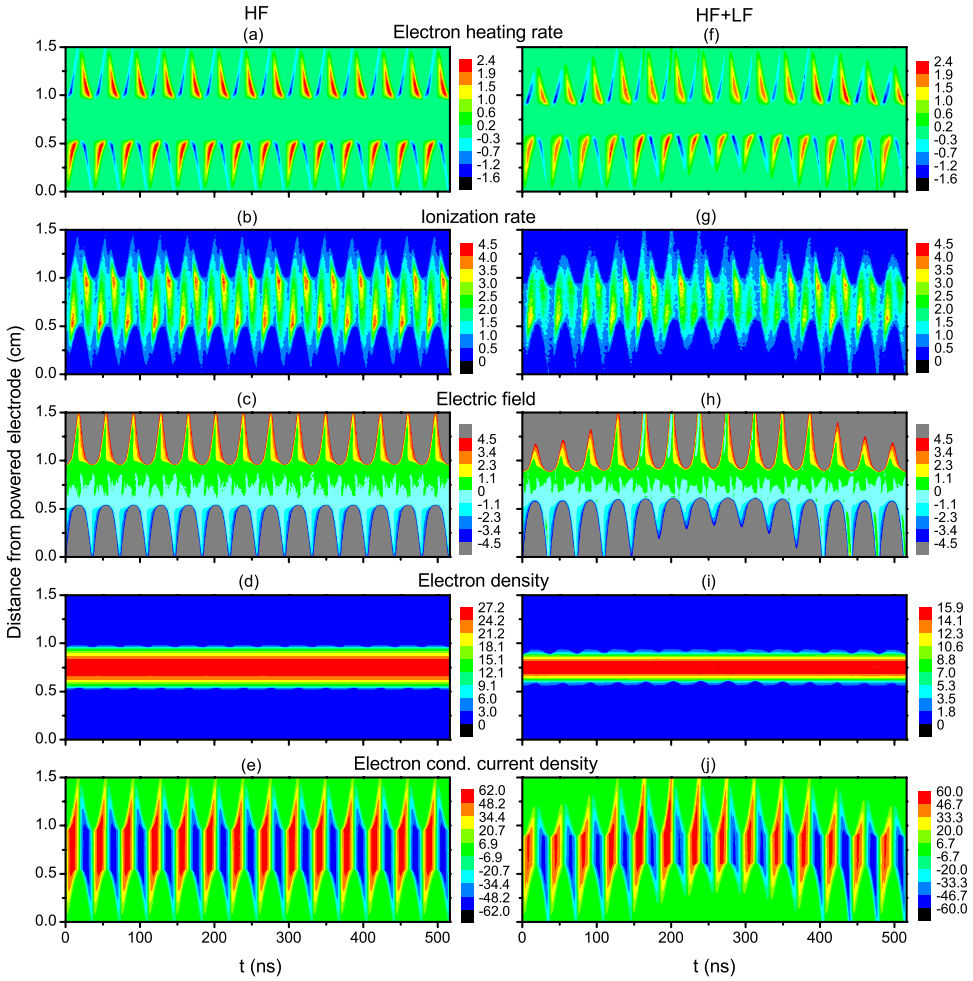

Figure 1. Spatiotemporal plots of the electron heating rate, ionization rate, electric field, electron density, and electron conduction current density for weakly electronegative plasmas (CF_4, 10 Pa, 1.5 cm electrode gap). First column (HF): single-frequency excitation at $f_{HF} = 27.12$ MHz, $V_{HF} = 300$ V. Second column (HF + LF): dual-frequency excitation at $f_{HF} = 27.12$ MHz, $V_{HF} = 300$ V + $f_{LF} = 1.937$ MHz, $V_{LF} = 100$ V. The colour scales are given in units of 10^5 W m^{-3} (heating rate), 10^{21} m^{-3} s^{-1} (ionization rate), 10^3 V m^{-1} (electric field), 10^{15} m^{-3} (electron density) and Am^{-2} (electron conduction current density).

the electron-neutral collision frequency, k is the Boltzmann constant, T_e is the electron temperature.

Here, it is found that the LF component affects the electron heating and ionization both in the bulk region and at the sheath edges via the following two frequency coupling mechanisms:

(i) The drift field, E_D, in the discharge center is influenced by the interaction of the HF and LF currents in the bulk, resulting in asymmetric electron heating and ionization patterns within one HF period. During the first half of the LF period, when the LF sheath expands at the powered electrode, at times of HF sheath expansion both RF sources cause electrons to be accelerated in the same direction (towards the grounded electrode). At times of HF sheath collapse the acceleration of electrons due to the HF component (towards the powered electrode) is opposite to that produced by the LF source. During the second half of the LF period, when the LF sheath collapses, constructive electron acceleration of the two RF sources (towards the powered electrode) takes place at times of HF sheath collapse, while at times of HF sheath expansion their effects on the electron motion are coupled in a destructive way. The result of this interaction is the asymmetric variation of the electron conduction current density, j, over each HF period, as can be seen in figure 2(j), and consequently, the variation of the strength of the drift electric field in the bulk. This, in turn, causes the electron heating and ionization due to E_D to be strong only at phases when the electron currents generated by the RF sources are both directed towards the same electrode. The modulation of the bulk electron density close to the sheath edges (figure 2(i)) is induced by the time modulated total ion density distribution in the bulk.

(ii) The development of the ambipolar field, E_A, at the sheath edge is affected by the modification of the sheath length by the LF source. The maximum electron density is always at the same position (around 0.25 cm and 0.4 cm in front of the electrodes in the SF and DF scenarios, in figure 2(d) and (i), respectively). Due to the LF voltage the sheath edge is pushed away from the electrodes and the sheath covers these positions at distinct times of maximum sheath width within the LF period. This results in the elimination of the electron density peaks at these phases,

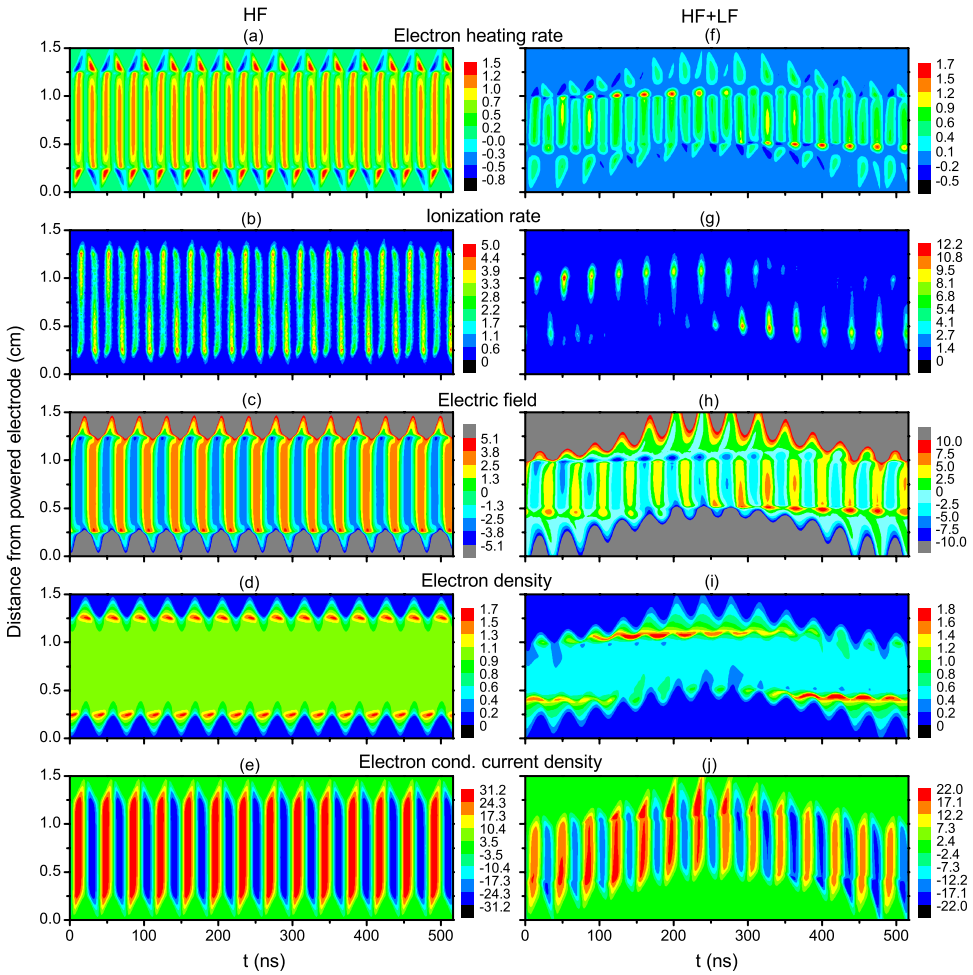

Figure 2. Spatiotemporal plots of the electron heating rate, ionization rate, electric field, electron density, and electron conduction current density for strongly electronegative plasmas (CF_4, 80 Pa, 1.5 cm electrode gap). First column (HF): single-frequency excitation at $f_{HF} = 27.12$ MHz, $V_{HF} = 100$ V. Second column (HF + LF): dual-frequency excitation at $f_{HF} = 27.12$ MHz, $V_{HF} = 100$ V + $f_{LF} = 1.937$ MHz, $V_{LF} = 200$ V. The units are the same as outlined in figure 1.

since essentially all electrons are pushed out of the sheaths at these times. The lack of local maxima and that of a strong gradient of the electron density prevents the development of a strong ambipolar field at these times. Consequently, electron heating caused by E_A and the related ionization at the collapsing HF sheath edge are observed only at phases when the sheath width is small and the position of the electron density peaks is not reached by the sheath edge at a given electrode.

Figure 3 shows the average energy of ions arriving at the electrodes, $\langle E_i \rangle$, their flux, Γ_i, and the electronegativity of the discharge as functions of the LF voltage amplitude, V_{LF}, for three different values of the HF voltage amplitude, V_{HF}, at 80 Pa. The trends of increasing $\langle E_i \rangle$ by increasing V_{LF} in figure 3(a), for all values of V_{HF}, as expected for a DF discharge, can be explained by the increase of the mean sheath voltage by applying a second voltage source. In case of $V_{HF} =$ 60 V, at $V_{LF} = 0$ V, the SF discharge is strongly electronegative and operates in the DA-mode. Here, the sheath length is small and the bulk region, confining the negative ions, is large. Applying an LF source, an increase of V_{LF} causes a pronounced increase of the sheath widths and causes the bulk to shrink. This forces the electronegativity to decrease, since negative ions are only present in the bulk (figure 3(c)). However, the electron heating and ionization in the reduced bulk region are enhanced by the constructive coupling of the two RF sources at distinct times of the LF period. Therefore, an increase of Γ_i is observed as a function of the LF voltage amplitude (figure 3(b)). Increasing V_{HF} to 100 V, the SF discharge operates in a hybrid α-DA mode, where significant ionization is induced by electrons heated by the sheath oscillations, as well as by those heated in the bulk region and at the collapsing sheath edge. An increase of V_{LF} results in larger sheath widths and a decrease of the electronegativity for high values of V_{LF}. Under such conditions the classical frequency coupling mechanisms affecting the sheath expansion heating and the novel coupling mechanisms affecting the DA-mode are both present. While the first mechanism causes Γ_i to decrease as a function of V_{LF} [28], the latter causes Γ_i to increase. For $V_{HF} = 100$ V both effects compensate each other resulting in an almost constant ion flux as a function of V_{LF}. In the case of $V_{HF} = 200$ V, the SF discharge operates also in hybrid α-DA mode, but most ionization is caused by electron beams generated by the sheath oscillations. Therefore, α-mode operation dominates over the

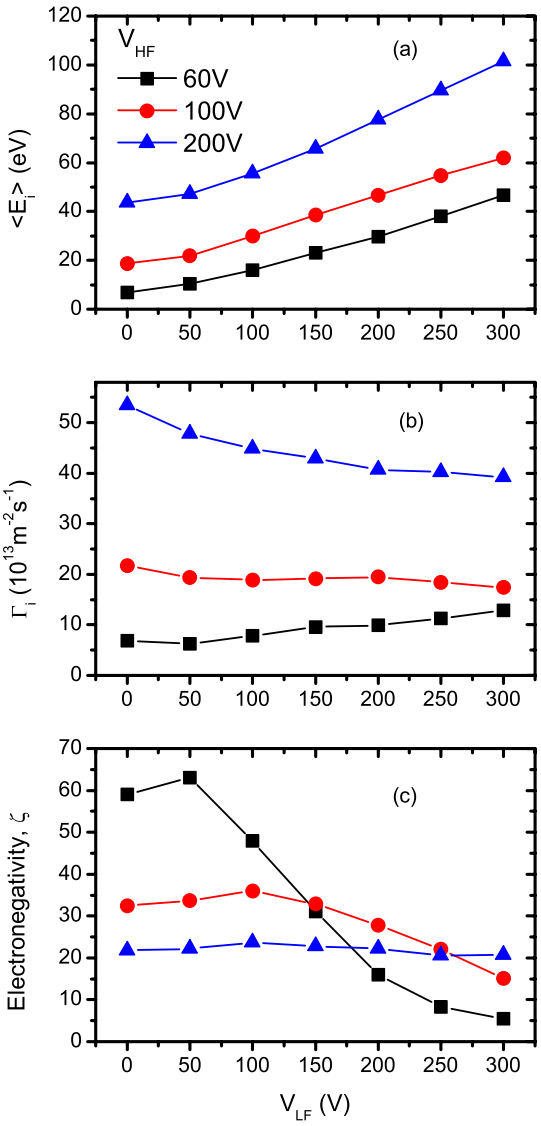

Figure 3. (*a*) Average ion energy, $\langle E_i \rangle$, (*b*) ion flux, Γ_i, at the powered electrode and (*c*) electronegativity as functions of the LF voltage amplitude, V_{LF}, for different values of the HF voltage amplitude, V_{HF}. Discharge conditions: CF_4, 80 Pa, $f_{HF} = 27.12$ MHz, $f_{LF} = 1.937$ MHz.

DA-mode. In this case, Γ_i decreases with increasing V_{LF} as a consequence of the classical frequency coupling mechanism depressing the electron heating and ionization at phases of a large LF sheath.

In conclusion, we have identified two novel coupling mechanisms in electronegative dual-frequency CCRF plasmas operated at substantially different frequencies affecting the electron heating (i) in the plasma bulk due to constructive/destructive interaction of drift electric fields originating from the HF and LF sources and (ii) at the collapsing sheath edge due to ambipolar electric fields influenced by the LF voltage amplitude via a modification of the sheath width. Based on a detailed kinetic analysis of these phenomena, their effect on the discharge operation and plasma parameters has been clarified. It is noted that these frequency coupling mechanisms are expected to be present in electronegative discharges operated in gases other than CF_4 as well, having consequences on the separate control of ion properties at the electrodes.

Acknowledgments

This work has been funded by the Hungarian Scientific Research Fund through the grant OTKA K-105476.

References

[1] Lieberman M A and Lichtenberg A J 2005 *Principles of Plasma Discharges and Materials Processing* 2nd edn (Hoboken, NJ: Wiley-Interscience)
[2] Makabe T and Petrović Z L 2006 *Plasma Electronics: Applications in Microelectronic Device Fabrication* (New York: Taylor and Francis)
[3] Chabert P and Braithwaite N 2011 *Physics of Radio-Frequency Plasmas* (New York: Cambridge University Press)
[4] Georgieva V and Bogaerts A 2005 *J. Appl. Phys.* **98** 023308
[5] Tong L Z and Nanbu K 2006 *Europhys. Lett.* **75** 63
[6] Shibata M, Nakano N and Makabe T 1995 *J. Appl. Phys.* **77** 6181
[7] Nakano N, Shimura N, Petrović Z L and Makabe T 1994 *Phys. Rev.* E **49** 4455
[8] Lisovskiy V A and Yegorenkov V D 2006 *Vacuum* **80** 458
[9] Boeuf J P 1987 *Phys. Rev.* A **36** 2782
[10] Gottscho R A 1987 *Phys. Rev.* A **36** 2233
[11] Liu Y X, Zhang Q Z, Liu J, Song Y H, Bogaerts A and Wang Y N 2012 *Appl. Phys. Lett.* **101** 114101
[12] Liu Y X, Zhang Q Z, Liu J, Song Y H, Bogaerts A and Wang Y N 2013 *Plasma Sources Sci. Technol.* **22** 025012
[13] Belenguer P and Boeuf J P 1990 *Phys. Rev.* A **41** 4447
[14] Hemke T, Eremin D, Mussenbrock T, Derzsi A, Donkó Z, Dittmann K, Meichsner J and Schulze J 2013 *Plasma Sources Sci. Technol.* **22** 015012
[15] Schulze J, Derzsi A, Dittmann K, Hemke T, Meichsner J and Donkó Z 2011 *Phys. Rev. Lett.* **107** 275001
[16] Kitajima T, Takeo Y, Petrović Z L and Makabe T 2000 *Appl. Phys. Lett.* **77** 849
[17] Boyle P C, Ellingboe A R and Turner M M 2004 *Plasma Sources Sci. Technol.* **13** 493
[18] Gans T, Schulze J, O'Connell D, Czarnetzki U, Faulkner R, Ellingboe A R and Turner M M 2006 *Appl. Phys. Lett.* **89** 261502
[19] Turner M M and Chabert P 2006 *Phys. Rev. Lett.* **96** 205001
[20] Schulze J, Gans T, O'Connell D, Czarnetzki U, Ellingboe A R and Turner M M 2007 *J. Phys. D: Appl. Phys.* **40** 7008
[21] Donkó Z 2007 *Proc. Symp. of Application of Plasma Processes (Podbanske, Slovakia, 20–25 January 2007)* ed J Matuska, S Matejčik and J D Skalny IL02 pp 21–4
[22] Kurihara M, Petrović Z L and Makabe T 2000 *J. Phys. D: Appl. Phys.* **33** 2146
[23] Georgieva V, Bogaerts A and Gijbels R 2004 *Phys. Rev. E* **69** 026406
[24] Bonham R A 1994 *Japan. J. Appl. Phys* **33** 4157
[25] Proshina O V, Rakhimova T V, Rakhimov A T and Voloshin D G 2010 *Plasma Sources Sci. Technol.* **19** 065013
[26] Donkó Z and Petrović Z L 2006 *Japan. J. Appl. Phys.* **45** 8151
[27] Schulze J, Derzsi A and Donkó Z 2011 *Plasma Sources Sci. Technol.* **20** 045008
[28] Schulze J, Donkó Z, Schüngel E and Czarnetzki U 2011 *Plasma Sources Sci. Technol* **20** 045007